Orissa Journal of Physics
ISSN 0974-8202

Vol. 22, No.2
August 2015
pp. 219-228

Ohmic resistance losses and their impact on efficiency in case of multicrystalline silicon solar cell

R.M. PUJAHARI[1, *] and M. C. ADHIKARY[2]

[1]Echelon Institute of Technology, Faridabad, India
[2]Dept. of Applied Physics and Ballistics, F M University, Balasore, India
[*]Corresponding author, E-mail: rpujahari@gmail.com

Received : *2.6.2015* ; *Accepted : 20.7.2015*

Abstract. Ohmic resistances play vital role in deciding the efficiency of the multicrystalline solar cells . In this paper a detailed analysis of the impact of various ohmic resistances like R_3 (the resistance of emitter between two grid fingers), R_5 (the resistance of the grid finger) and R_6 (the resistance of collection bus) using three dimensional (3D) SS screen printed solar cell for front silver metallization of multicrystalline large area is analysed. For the fabrication of large area (125 mm $\times$125 mm) high efficiency (>15%) crystalline silicon solar cells are used and analysed. This paper reports the high efficiency of the 3D screen printing to enhance the solar cell efficiency upto 15.6% in the production plant.

Keywords. mc-Si silicon solar cell texturization, Screen printing 3D mesh, Telestep profile of Ag- grid fingers, cell LIV and DIV characteristics

1. Introduction

In commercial large area crystalline silicon PV plants, different metallization schemes such as photolithography after vacuum evaporation, electroplating, and buried contact are used, they are more expensive as well as time consuming for large scale production process [1]. Screen printing technique provides a cost-effective alternative to those complicated schemes due to which it has already been a widespread method in solar cell industries [2]. For crystalline silicon, the well established metallization method is screen printing technology which results in the surface covered with suitable metal pastes. However, for metallization of the emitter surface, it is very much required to control the series resistance loss after cell fabrication. The main problem that is generally experienced in screen printing metallization is poor contact quality that results in poor fill factor of the fabricated cells. Metal contact with silicon surface depends on several parameters such as surface condition, emitter surface concentration

and dopant impurity profile [3], anti-reflection coating on the emitter surface, screen parameters, metal pastes and above all, the firing profile. Optimization of front and back contacts for the solar cell is the ultimate task for process designers. People thus look for an approach which not only reduces the effects of series resistance by enhancing the cell fill factor (FF), but also yields a higher short circuit current (I_{sc}) by the reduction of the shadowing loss without compromising with production output.

In our present work, multicrystalline silicon solar cells are fabricated in a conventional industrial process. During cell front screen printing both the two dimensional (2D) and three dimensional (3D) stainless steel meshes are used. Our paper reports the impact of these screen printing processes on the performance of electrical parameters of the solar cell by studying illuminated voltage – current (LIV) and dark voltage – current (DIV) characteristics to ascertain the superiority of the 3D screen. Also knitting of the meshes and surface reflectivity of the cells are studied by the optical microscope and the spectrophotometer respectively.

2. Experimental

A. Cell fabrication

The starting material for the experiment is boron doped p-type mC-Si wafers of base resistivity 0.5 ~ 3.0 Ω-cm of brand SOLSIX from Deutsche Solar of size 125 mm × 125 mm square. and cells are fabricated using texturization with sodium hydroxide (NaOH) – sodium hypochlorite (NaOCl) based polishing solution [4]. The alkali based polishing solution has NaOH solution (20% by weight) and NaOCl solution in the ratio of 1:1 by volume [5]. The polishing bath (made with SS316 material) is filled with this solution and is heated by teflon heater (jacket type) from the bottom and a constant temperature of 80-82^{o}C is maintained with the combination of thermocouple and PID controller. 40 wafers are loaded in a single teflon jig and the single polishing bath of NaOH-NaOCl solution can accommodate 6 jigs, i.e., 240 wafers at a time for 20 minutes. In the same solution of NaOH-NaOCl bath 10 batches, i.e., 2400 wafers are polished. Heating of the solution is required only for the first batches for bath temperature to reach up to 82^{o}C, and later further heating for subsequent polishing batches are not required due to slow exothermic nature of silicon polishing reaction [6]. After texturing, the wafers are then doped with phosphorus (P) using optimized diffusion condition with phosphorus oxychloride as the source at 875^{o}C. After diffusion, the phosphosilicate glass (PSG) layer is removed in dilute hydrofluoric

(HF) acid solution. The low temperature oxidation (LTO) is a pre requisite step to dissolve hard PSG which cannot be removed by HF. Thermal SiO_2 of thickness ~150-200 Å is grown on the sample surface at 750^0C. After LTO, the grown oxide is again removed so that it consumes some dead layer to enhance cell blue response [7]. The P-impurities diffused on the edges of the wafer need to be removed to prevent shunting in the wafer and to minimize the leakage current. In our cost effective process, the stack of wafers are edge-etched together using HF-nitric (HNO_3)-acetic (CH_3COOH) solution in 3:5:3 ratio for 1 min at 7-8˚C bath temperature. In order to suppress reflections from a solar absorber surface an anti-reflection coating (ARC) layer is deposited on top of the solar wafer. For the AR coating to function well it should be made of a material having a lower refractive index than the underlying surface. ARC is particularly beneficial for multicrystalline material that cannot be easily textured. In our process ARC of 700Å of Si_3N_4 of refractive index 2.05 has been deposited at 450˚C by plasma enhanced chemical vapour deposition. The back and front sides are screen printed with silver-aluminium (DUPONT PV202), aluminium (DUPONT PV333) and silver pastes (DUPONT PV145) one by one, followed by baking of individual pastes of the printed wafers. For excellent screen printed metallization we require the setting of the optimum conditions for the paste, optimized screen mask specifications and optimized printing conditions. After depositing, the layer is sintered at temperatures of approximately >760^{o}C in a conveyer belt furnace. The complete process flow chart is given in Fig.1.

B. Metallization

For the front emitter metallization, two batches of 40 wafers each, are taken after back aluminium and silver-aluminium printing. First 40 wafers are then screen printed on the front surfaces by 2D 325 and the other 40 wafers by 3D SS 325 screens [13, 14]. After printing and cofiring, one cell from each batch is taken as the representative for the 2D and 3D screen printing processes.

C. Characterization

Small pieces of dimension 2 cm ×2 cm are cut from the representative cells of 2D and 3D screen printing categories by using Nd–YAG laser for the surface reflectance analysis by spectrophotometer[15]. Before the surface analysis, wafer pieces (as samples) are cleaned ultrasonically in isopropyl alcohol followed by rinsing in DI water and drying. These samples containing only the grid lines are taken from the same areas of both the cells. The DIV and LIV characteristics of

the cells are also measured. Their LIV characteristics are measured under 1 SUN intensity with AM1.5 Global spectrum[16].

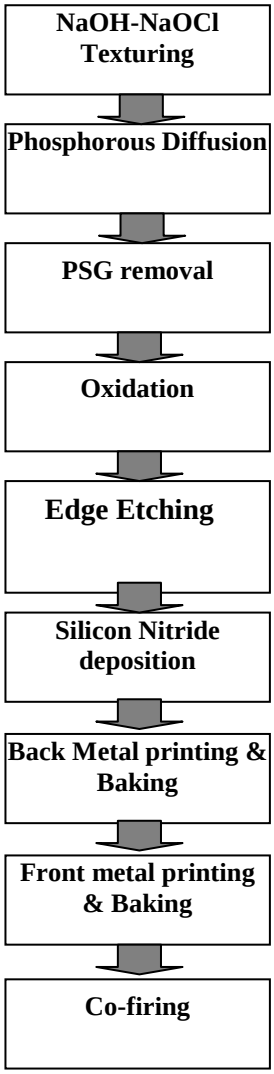

Fig.1. Solar Cell Fabrication

3. Results and discussion

The figure 2(a) shows the ohmic resistance in a solar cell. The individual resistances are R_1 (the metal- semiconductor contact on total back surface), R_2

(the semiconductor material i.e. base resistance), R_3 (the resistance of emitter between two grid fingers), R_4 (the resistance of metal semiconductor contact on the grid finger), R_5 (the resistance of the grid finger) and R_6 (the collection bus).

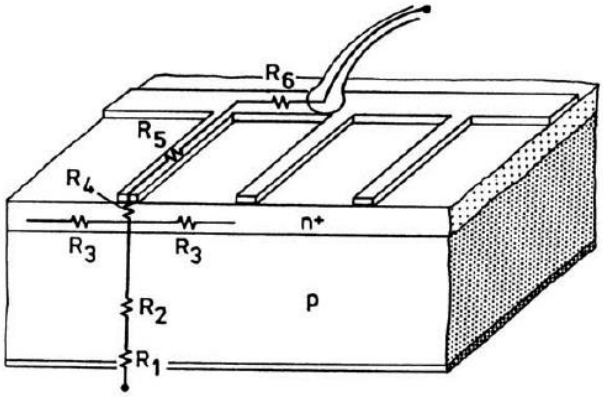

Fig.2(a). Series resistance in a Solar cell

The total series resistance(R_s) is found by linking the individual resistance values R_1 to R_6 together in a suitable resistance network.

If in detail the contribution of all resistances are calculated in details then $R_1$and R_2 can be disregarded in all practical cases. If the contact material and the finger width are correctly selected, then R_4 also makes no significant contribution. The resistance R_3, R_5 and R_6 primarily determines the R_s.

The resistance R_3 is expressed as in equation(1),

$$R_3 = \frac{R_\square}{l}\frac{d}{6} \tag{1}$$

Where $R_\square$ is designated sheet resistance which is measured in Ω/□ i.e. ohms / square, l is length of the grid finger and d is distance between two grid fingers.

The resistance R_5 is calculated by the formula as given below:

$$R_5 = \frac{1}{3}\rho_{met}\frac{l}{aL} \tag{2}$$

In the above equation (2) l is the length, L is the width and a is the thickness of the finger. So also $\rho_{met}$is the resistivity of the metal.

Similarly the calculation of R_6 can be measured by the following equation (3):

$$R_6 = \frac{1}{3\times 2}\frac{l_B}{aL_B}\rho_{met} \tag{3}$$

Where l_B is the total length of the busbar, L_B is the width of the busbar, a is the thickness of the finger and $\rho_{met}$is the resistivity of the metal.

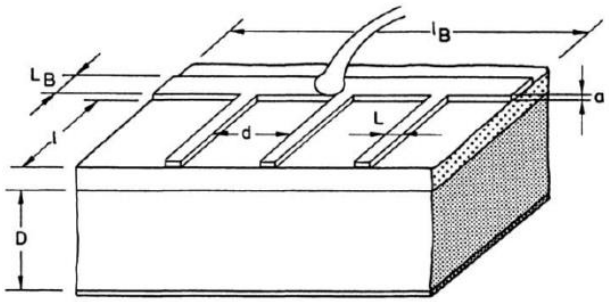

Fig.2(b). Structure of the contact grid in a Solar cell

Fig.3 indicates telestep profiles of two consecutive Ag-grid fingers for a 3DSP cell in a single scan. We have l = 118 mm from our grid design data and $R_{\square}$= 5mΩ/□ [10]. So for the 3DSP cell value of R_3 is calculated as 0.1659mΩ taking d = 2.35mm. Fig.4 is the telestep profiles of Ag-grid fingers of cells. From the experimental data from Fig. 4. the obtained values of R_3 is 0.1659mΩ.

All the experimentally determined screen printed parameters from Fig.4 are listed in Table-I. From the Table-I, using ρ_{met}= 4.8x10-10Ω-m[11], in eqn.(2) the value of R_5 is calculated as 7.99mΩ. For the 3DSP cell, with the experimental value from Table-I the value of R_5 is calculated as 7.01mΩ taking l = 118mm, a = 15.03μm, L = 179μm[12-15]. Theoretical value of R_s is calculated by adding R_3 and R_5 and the values for R_s is 7.1mΩ for the 3DSP cell.

The values of R_s as obtained in Table-I is 7.1 mΩ which is very close to the experimental values[16]. This indicates that the experimental data for the height and width of finger ascertains that the series resistance values of the 3DSP cells is quite accurate as required[17].

Table 1. 2DSP and 3DSP Screen Printed Parameters as Measured by Stylus.

Screen used	d **(mm)**	a **(μm)**	L **(μm)**	R_3 **(mΩ)**	R_5 **(mΩ)**	R_s **(mΩ)**
3D	2.37	15.03	179	0.1659	7.01	7.1

The contribution of shadowing loss has also been analysed in the context of 3D screen printed cells. There are 55 lines in a typical 125 X 125 mm square cell[18-19]. Approximate lengths of the lines are 121mm. Ag metal coverage for the 3DSP cell from the emitter surface is 121 mm x 179 μm[20]. This shows a percentage reduction in shadowing loss of 0.7% in case of 3DSP cell.

A major impact of excellent emitter metallization is clearly visible in the significant improvement in FF of the 3DSP cell[21]. This up gradation of the I_{sc} and FF results into an improvement of cell efficiency to 16% (3DSP) without any major variation in cell fabrication techniques.

The increase in metal heights during the 3D screenprinting of the emitter surface layer is quite large[22]. Higher height of front silver decreases both the shadowing loss and metal resistance. It resulted into a marginal decrease of reflectivity by 0.13% in 300 nm to 1200 nm wavelength range. The value of R_s obtained after calculating R_3 and R_5 as 7.1 mΩ for 3DSP cells which is quite close to the experimental values 7.3mΩ. Low series resistance value (7.1mΩ) of the 3DSP cell enhances cell FF upto 0.764[23]. In case of 3DSP cell there is a reduction of shadowing loss upto an extent of 0.7% which is also responsible for the increase in the cell efficiency.In a cumulative effect the cell efficiency enhances from 14.7% to 15.5% without any other change in the regular production line. Also higher height eases soldering with solder plated copper strip and creates strong bonding between them at tabbing step during module fabrication.

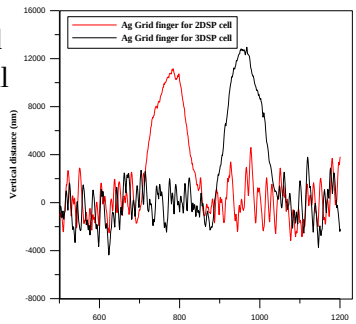

Fig. 3 Telestep Profiles of Ag-grid Fingers 3DSP cells

The reflectivity comparison graph is shown in Fig.4. There is a definite marginal decrease in average reflectivity to 14.47% in the wavelength range of 300 nm to 1200 nm which is contributed by the increase in finger height in the 3D printing [24]. This small enhancement of the reflectivity is also caused by the marginal shadowing loss minimization in the 3D screen and this fact contributed to the increase of short circuit current of the cell as shown in the LIV characteristics in Fig.5. The uniformity of

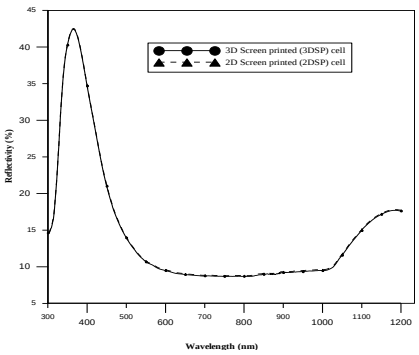

Fig.4. Variation of surface reflectance of the front surface of the 3DSP cell.

metal coverage in the 3DSP cell is ascertained by the comparison of the cell LIV parameters as shown in Table-II[25]. A major impact of excellent emitter metallization is clearly visible in the significant improvement in FF of the 3DSP cell. This upgradation of the I_{sc} and FF results into an improvement of cell efficiency to 15.6% (3DSP).

Also the LIV and DIV characteristics of the cells (shown in Fig.5 and Fig. 6 respectively) have been shown in this figures and thus indicates no notable change in cell leakage current characteristics.

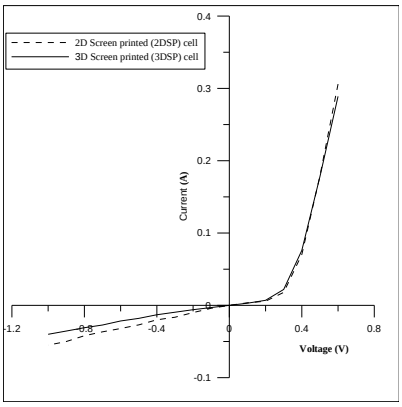

Fig.5 The illuminated current – voltage (LIV) characteristics curves of the 3DSP cells.

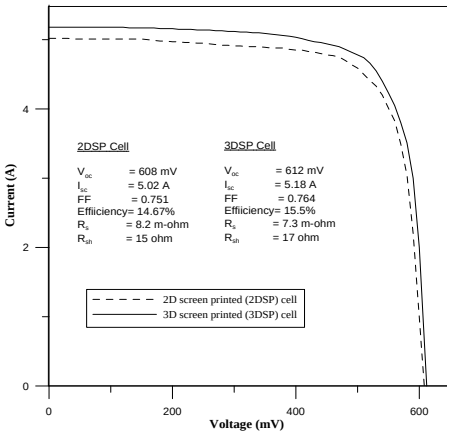

Fig.6. The DIV characteristics curves of 3DSP cell

Table-II: Electrical parameters of solar cell fabricated using 3D screens

Screen used	**V_{oc} (V)**	**I_{sc} (A)**	**FF**	**R_s (mΩ)**	**R_{sh} (Ω)**	**Efficiency (η), %**
3D	0.612	5.18	0.764	7.3	17	15.6

4. Conclusion

The increase in metal heights during the 3D screen printing of the emitter surface layer is quite large. Higher height of front silver decreases both the shadowing loss and metal resistance[25]. It resulted into a marginal decrease of reflectivity by 0.13% in 300 nm to 1200 nm wavlength range. Low series resistance value (7.3 mΩ) of the 3DSP cell enhances cell FF upto 0.764. In a cumulative effect the cell efficiency enhances to 15.6% without any other change

in the regular production line. Also higher height eases soldering with solder plated copper strip and creates strong bonding between them at tabbing step during module fabrication. This clearly reflects the high efficiency of the fabrication process.

Acknowledgements

The authors express their sincere thanks to P.G. Dept. of Applied Physics and Ballistics, FM University, Balasore, India for continuous stimulation and support for the present research.

References

[1] A. Ebony, Y. H. Cho, M. Hilalii, A. Rohatgi and D. Ruby; *Solar Energy Materials and Solar Cells*, **74**, 51 (2002).

[2] M. Bohm, E. Urbanski, A. E. Delahoy and Z. Kiss; *Solar Cells*, **20**, 155 (1987).

[3] P.K.Basu, B.C.Chakravarty, S.N.Singh, P.Dutta and R.Kesavan, *Solar Energy Materials and Solar Cells*, **43**, 15 (1996).

[4] U.Gangopadhyay, S.K.Dhungel, P.K.Basu, S.K. Dutta, H.Saha and Junsin Yi, *Solar Energy Materials and Solar Cells*, **91**, 285 (2007).

[5] P.K.Basu, H. Dhasmana, D. Varandani, B.R. Mehta and D.K. Thakur, *Solar Energy Materials and Solar Cells*, **93**, 1743 (2009).

[6] P.K.Basu, H. Dhasmana, Udayakumar N. and D.K. Thakur, *Renewable Energy*, **34**, Nov. 2009, p.2571-2576.

[7] J.Lindmayer and J.F.Allison, COSMAT Tech. Rev., **3,** 1 (1973).

[8] www.teiko-sino.com

[11] E. Vazsonyi, Z. Vertesy, A. Toth and J. Szlufcik, *Journal of Micromechanics and Microengineering*, **13**, 165 (2003).

[12] U. Gangopadhyay, S.K. Dhungel, P.K. Basu, S.K. Dutta, H. Saha and Junsin Yi, *Solar Energy Materials and Solar Cells*, **91**, (2007), 285 (2007).

[13] M.C. Adhikary, R.M. Pujahari, *Journal of Energy and Power Resources.ISSN:Print-2333-9136,Online-2333-9144(2014)*

[14] P. K. Basu, R.M. Pujahari, Harpreet Kaur, Devi Singh, D. Varandani and B.R. Mehta, *Solar Energy, **84**(2010)1658-1665*, Elsevier.

[15] R. M. Pujahari , M C Adhikary, *ISST Journal of Applied Physics.ISSN:0976-903X*, ***Vol-5** No.1(2014)*

[16] D. Singh, R.M. Pujahari, Harpreet Kaur and P. K. Basu *ISST Journal of Applied Physics.ISSN:0976-903X*, **Vol-1(2),** 9 (2010).

[17] R.M. Pujahari, M. C. Adhikary, 12th *International Congress on Renewable Energy (ICORE-2014), ISBN: 978-81-8454-150-2*, Manekshaw Centre, New Delhi, Organised by Solar Energy Society of India, Dec. 8-9, p.251 (2014).

[18] M. C. Adhikary, R.M Pujahari *International Congress on Renewable Energy (ICORE-2013), ISBN: 978-93-82880-80-6*, KIIT University, Bhubaneswar, Organised by Solar Energy Society of India, Nov. 27-29, p.181-186 (2013)..

[19] R.M. Pujahari, Devi Singh, and P. K. Basu, *International Conference on Applications of Renewable Energy Utilization (ICREU-2012)*, Coimbatore Institute of Technology, Coimbatore, Tamil Nadu, India, Jointly with Oklahoma State University, Stillwater, USA, January 4-6,p-4-5 , 2012.

[20] R.M. Pujahari, Devi Singh, and P. K. Basu, *International Conference on Applications of Renewable & Sustainable Energy(REIS-2010),*Department of Physics, Under UGC SAP Programme, Osmania University, Hyderabad, December 16-18, , 2010.

[21] R.M. Pujahari, Harpreet Kaur, Devi Singh, and P. K. Basu, *International Conference on Renewable Energy (ICARE-2010), ISBN : 13978-81-909984-0-6*, Maulana Azad National Institute of Technolgy, Bhopal, June 26-28, Vol.1, p-157-162, 2010.

[22] R.M. Pujahari, Harpreet Kaur,Devi singh, and P. K. Basu, *4thInternational Multiconference on Intelligent Systems & Nanotechnology(IISN-2010),*p-211-214, Feb 26-28,Institute of Science and Technology, Klawad, Haryana, 2010.

[23] Hrishikesh Dhasmana, N. Udaykumar, Sunil Bist, Ravi Malik, R.M.Pujahari, Devi Singh and P.K.Basu, *15th. International workshop on The Physics of Semiconductor Devices (IWPSD-2009) ISBN: 978-93-80043-55-5*, Dec 15-19, Photovoltaics-p11-13, 2009. (*Awarded best poster in the PV section*)

[24] R.M. Pujahari, Harpreet Kaur, Devi Singh, and P. K. Basu, *International Conference on Renewable Energy (ICARE-2010), ISBN : 13978-81-909984-0-6*, Maulana Azad National Institute of Technolgy, Bhopal, June 26-28, Vol.1, p-157-162, 2010.

[25]R.M. Pujahari, Devi Singh, and P. K. Basu, *National Conference on Sustainable Development in Energy Sector*, University of Petroleum & Energy Studies, Dehradun, Uttarakhand, India, Jointly with World Energy Council, Indian Committee Member, 8-9, April, p-20, 2011. Tajima K, Hironaka M, Chen K, Nagamatsu Y, Kakigawa H, Kozono Y. Dental Materials Journal **27**, 258 (2008).